Lab on a Chip

Accepted Manuscript

This is an *Accepted Manuscript*, which has been through the Royal Society of Chemistry peer review process and has been accepted for publication.

Accepted Manuscripts are published online shortly after acceptance, before technical editing, formatting and proof reading. Using this free service, authors can make their results available to the community, in citable form, before we publish the edited article. We will replace this *Accepted Manuscript* with the edited and formatted *Advance Article* as soon as it is available.

You can find more information about *Accepted Manuscripts* in the **Information for Authors**.

Please note that technical editing may introduce minor changes to the text and/or graphics, which may alter content. The journal's standard **Terms & Conditions** and the **Ethical guidelines** still apply. In no event shall the Royal Society of Chemistry be held responsible for any errors or omissions in this *Accepted Manuscript* or any consequences arising from the use of any information it contains.

Lab on a Chip

ARTICLE

Rapid imaging, detection and quantification of *Giardia lamblia* cysts using mobile-phone based fluorescent microscopy and machine learning

Hatice Ceylan Koydemir[a], Zoltan Gorocs[a], Derek Tseng[a], Bingen Cortazar[a], Steve Feng[a], Raymond Yan Lok Chan[a], Jordi Burbano[a], Euan McLeod[a], and Aydogan Ozcan*[abc]

Rapid and sensitive detection of waterborne pathogens in drinkable and recreational water sources is crucial for treating and preventing the spread of water related diseases, especially in resource-limited settings. Here we present a field-portable and cost-effective platform for detection and quantification of *Giardia lamblia* cysts, one of the most common waterborne parasites, which has a thick cell wall that makes it resistant to most water disinfection techniques including chlorination. The platform consists of a smartphone coupled with an opto-mechanical attachment weighing ~205 g, which utilizes a hand-held fluorescence microscope design aligned with the camera unit of the smartphone to image custom-designed disposable water sample cassettes. Each sample cassette is composed of absorbent pads and mechanical filter membranes; a membrane with 8 μm pore size is used as a porous spacing layer to prevent the backflow of particles to the upper membrane, while the top membrane with 5 μm pore size is used to capture the individual *Giardia* cysts that are fluorescently labeled. A fluorescence image of the filter surface (field-of-view: ~0.8 cm^2) is captured and wirelessly transmitted via the mobile-phone to our servers for rapid processing using a machine learning algorithm that is trained on statistical features of *Giardia* cysts to automatically detect and count the cysts captured on the membrane. The results are then transmitted back to the mobile-phone in less than 2 minutes and are displayed through a smart application running on the phone. This mobile platform, along with our custom-developed sample preparation protocol, enables analysis of large volumes of water (e.g., 10-20 mL) for automated detection and enumeration of *Giardia* cysts in ~1 hour, including all the steps of sample preparation and analysis. We evaluated the performance of this approach using flow-cytometer-enumerated *Giardia*-contaminated water samples, demonstrating an average cyst capture efficiency of ~79% on our filter membrane along with a machine learning based cyst counting sensitivity of ~84%, yielding a limit-of-detection of ~12 cysts per 10 mL. Providing rapid detection and quantification of microorganisms, this field-portable imaging and sensing platform running on a mobile-phone could be useful for water quality monitoring in field and resource-limited settings.

Introduction

Providing access to safe drinking water, supplying adequate sanitation services, and promoting better hygiene practices are important goals to eliminate water-related diseases worldwide[1]. Despite tremendous improvements over the past several decades, there are still more than two billion people who lack access to improved sanitation facilities and more than half a billion people who live with unimproved drinking water sources, especially in developing parts of the world[2], which account for more than one-third of the total world population[3]. Moreover, even developed countries are facing emerging problems such as limited financial resources, urbanization, and population growth that altogether increase the occurrence of waterborne diseases. Accordingly, waterborne pathogens (e.g., bacteria, viruses, and parasites) pose significant risks to human health worldwide, primarily through diarrhea (*affecting four billion people each year*), and can impose significant economic burden and increased healthcare costs on countries[4]. Therefore, rapid, sensitive, and cost-effective detection of contaminated water sources is an important step to prevent waterborne diseases and their spread[5].

Among various waterborne pathogens, *Giardia lamblia* (*G. lamblia*) is one of the most common intestinal protozoan

parasites that remains difficult to eliminate using traditional methods (e.g., chlorination)[6,7] due to its thick cell wall. Conventional methods commonly used in water analysis laboratories for detection and enumeration of this parasite depend on filtration of several liters of water, immunomagnetic separation of cysts from debris, and fluorescence detection of cysts using bench-top microscopes[8]. These methods offer high sensitivity and specificity but are time-consuming (requiring e.g., 1-2 days), need trained specialists to operate bulky and relatively expensive equipment, and are prone to human errors. Various other detection methods[9–18] such as e.g., Polymerase Chain Reaction (PCR)[9,12], flow cytometry[12], and hollow-fiber ultrafiltration in combination with heat dissociation[16], have also been developed to partially mitigate some of these disadvantages. These methods, however, are either too complex to operate in a field-portable design or cannot process large sample volumes (e.g., 10 mL) and therefore, they are impractical to use in resource-limited environments for rapid analysis of large volumes of water samples.

Here we present an alternative smartphone-enabled platform for rapid (i.e., ~1 hr) detection and counting of intact *G. lamblia* cysts in water samples. In this work, we focused on intact cyst capture and counting rather than detection of cyst fragments since the ingestion of intact cysts causes Giardiasis. The opto-mechanical attachment to the smartphone weighs only 205 g and is composed of a disposable custom-designed sample cassette capable of holding large volumes (i.e., 20 mL) of water sample to be analyzed, and a cost-effective mobile fluorescence microscope that has a wide FOV of ~0.8 cm² (see Figure 1). This fluorescence microscope component consists of a 3D-printed housing that aligns with the existing camera module of

the smartphone, an external lens, an excitation filter, an emission filter, eight light-emitting-diodes (LEDs), a mechanical z-stage, and two batteries. The main components of our sample cassette consist of absorbent pads and two different filter membranes, with 8 µm and 5 µm pore sizes, respectively (see Figure 1d). The larger pore membrane works as a spacing layer to prevent the backflow of particles native to the absorbent pads to the upper membrane, while the smaller 5 µm pore size membrane is used to capture the labeled *Giardia* cysts. For a given water sample of interest, our sample processing starts with fluorescently labeling the test solution, and then filtering it through our custom-designed cassette, after which the cassette is placed at the back of our smartphone microscope attachment for fluorescent imaging. *Giardia* cysts that are captured at the surface of the filter membrane are illuminated by eight LEDs, uniformly exciting the entire membrane as illustrated in Figure 1e. After its capture, the fluorescence image is wirelessly transmitted using a custom-designed smart application (*Giardia* Analyzer) to our servers for rapid and automated counting of the labeled cysts. The digital analysis of the mobile-phone image is based on a machine learning algorithm that is trained on statistical features of *Giardia* cyst images so that it can automatically and specifically recognize cyst signatures from other (auto)fluorescent micro-objects that are non-specifically captured on the filter membrane. The result of this machine learning based analysis of each fluorescence image is returned back to the same mobile-phone within ~2 min, and is displayed to the user through the same *Giardia* Analyzer smart application.

We tested the performance of this automated detection
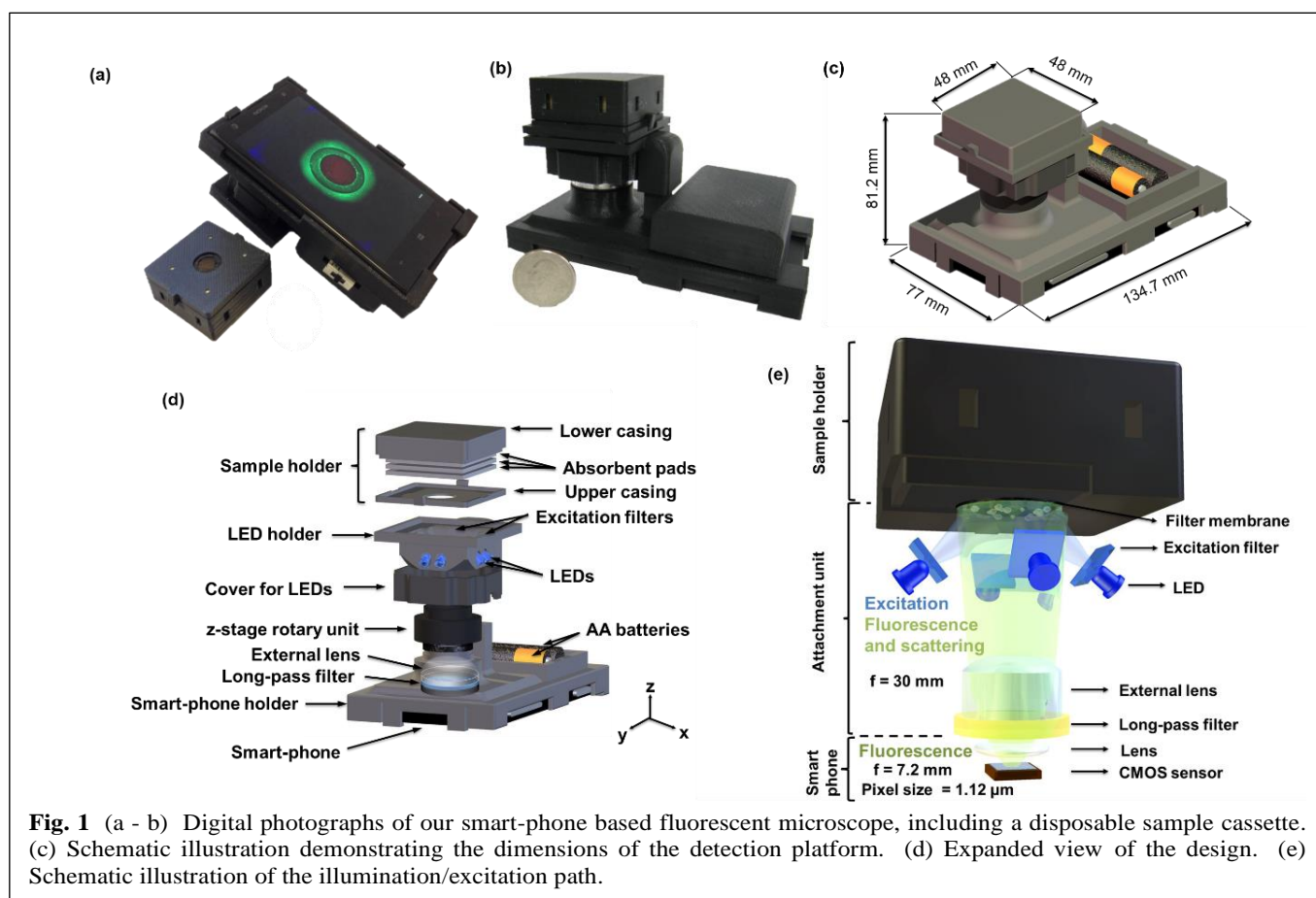
Fig. 1 (a - b) Digital photographs of our smart-phone based fluorescent microscope, including a disposable sample cassette. (c) Schematic illustration demonstrating the dimensions of the detection platform. (d) Expanded view of the design. (e) Schematic illustration of the illumination/excitation path.

platform using flow cytometer-enumerated *G. lamblia*-spiked water solutions, where each test takes ~1 hour to run, including labeling, filtering, imaging and cyst counting steps. Our experiments demonstrated an average cyst capture efficiency of ~79% along with an automated cyst counting sensitivity of ~84%, which together yielded a limit of detection (LoD) of ~12 cysts per 10 mL. This field-portable fluorescent microscopy platform that is integrated on a mobile-phone, together with its machine learning based digital image processing framework, can provide a valuable solution for automated and rapid detection of various waterborne pathogens, in addition to *Giardia* cysts, even in remote and resource limited settings.

Materials and Methods

Materials

Hydrophilic polycarbonate black filter membranes (pore size = 5 μm) (product no. PCTB5013100) were purchased from Sterlitech Corp. (Kent, WA, U.S.A.). Nuclepore track-etched polycarbonate membranes (pore size = 8 μm) (product no. 110414) were purchased from GE Healthcare Life Sciences (Pittsburgh, PA, U.S.A.). The absorbent pads (product no. 28297-988) were purchased from VWR (Visalia, CA, U.S.A.). Black masking tape (product no. T743-1.0) and lens tube (product no. SM1L03) were purchased from Thorlabs (Newton, NJ, U.S.A.). Luer caps (product no. FTLLP-1) were purchased from Value Plastics (Fort Collins, CO, U.S.A.). Disposable syringes with BD Luer-Lok™ tip (product no. 309604) were purchased from BD Company (Franklin Lakes, NJ, U.S.A.). Sprayon® epoxy paint (product no. 4190965) was purchased from Chase Products Co. (Broadview, IL, U.S.A.).

Tween® 20 (product no. P9416) and reagent water (product no. 320072) were purchased from Sigma Aldrich (St. Louis, MO, U.S.A.). Isopropanol (product no. A416P-4) was purchased from

Fisher Scientific (Pittsburgh, PA, U.S.A.). Anti-*Giardia* reagent fluorescein labelled stain (product no. *Giardia*-a-Glo™, A300FLK-20X), bulk parasite suspension (1% formalin fixed) (product no. P101), *Giardia* spiked suspensions enumerated by flow cytometer and fixed using 1% formalin (product no. PACIR), wash buffer (product no. WB101), dilution buffer (product no. B100-20), anti-fading mounting media (product no. M101), and counterstain (product no. C101) were purchased from Waterborne Inc. (New Orleans, LA, U.S.A.) and stored at 4 °C. The aspherized achromatic lens (*f* = 30 mm) (product no. 49-662) was purchased from Edmund Optics (Barrington, NJ, U.S.A). The long-pass filter (product no. FF01-500/LP-23.3-D) was purchased from Semrock Inc. (Rochester, NY, U.S.A.). LEDs (product no. 516-2800-1-ND) and double sided adhesive tape (product no. 3M9720-ND) were purchased from Digi-Key Corporation (Thief River Falls, MN, U.S.A.). Excitation filter (product no. ET470/40x) was purchased from Chroma Inc. (Bellows Falls, VT, U.S.A.).

Preparation of solutions

Before preparing water samples for analysis, we need to prepare two solutions for our experiments: a diluted antibody-based fluorescein-labelled stain and a 0.01% Tween® 20 solution in reagent water. The diluted stain solution is used for labeling of the *Giardia* cysts in the water sample while the Tween® 20 solution is used to reduce the adhesion of the *Giardia* cysts onto the walls of the delivery syringe barrel in order to increase the *Giardia* cyst recovery rate of our system.

To prepare the diluted stain, a concentrated anti-*Giardia* reagent fluorescein labelled stain (i.e. 20X) is diluted to 1X using the dilution buffer provided by the manufacturer with a ratio of 19:1 in an Eppendorf tube and mixed. In order to prepare 0.01% Tween® 20 solution, 5 μL of Tween® 20 is added into 50 mL of reagent water in a falcon tube and dissolved by vortex mixing at 10,000 rpm for five minutes. All solutions require storage at 4 °C following their
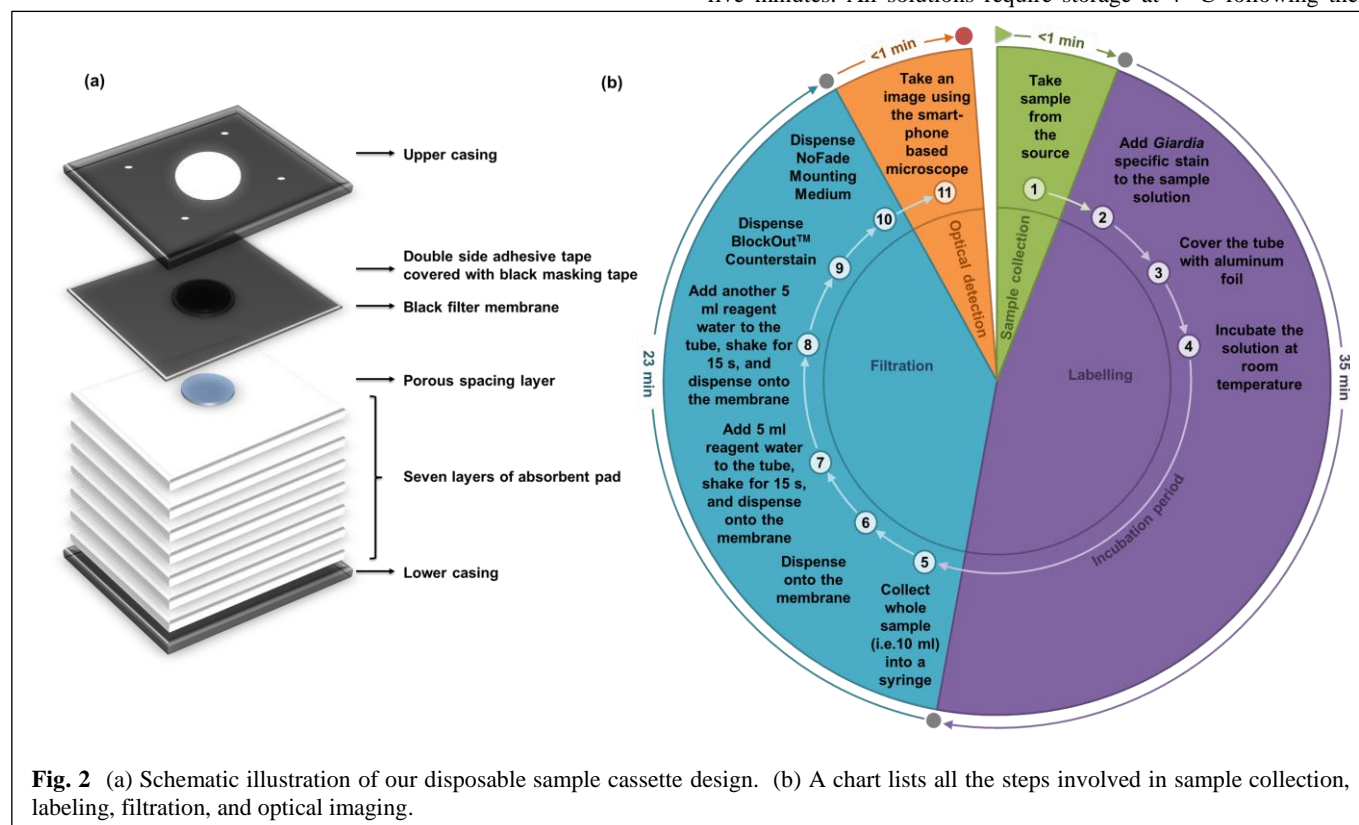
Fig. 2 (a) Schematic illustration of our disposable sample cassette design. (b) A chart lists all the steps involved in sample collection, labeling, filtration, and optical imaging.

preparation.

Sample cassette assembly and preparation

To be able to process large volumes of water samples, we designed a disposable sample holder that can be easily fabricated in large quantities using low cost materials including e.g., cotton absorbent pads and porous filter membranes. This sample holder (Figure 2a) consists of a custom-designed and 3-D printed casing, absorbent pads, a porous spacing layer, a black filter membrane, and tape. The lower and upper casings of the disposable sample holder were printed on a 3-D printer (Stratasys, Dimension Elite) using acrylonitrile butadiene styrene (ABS) material. The lower casing contains holes to increase airflow and allow the absorbent pads to more quickly soak up the water sample of interest. We use the lower casing as the housing of the interior components of the sample holder and the upper casing as a cap to fix the sample holder to the backside of the smartphone microscope attachment. By increasing or decreasing the number of pads used, it is possible to change the volume of sample water that can be processed using this sample holder. For example, in our design we use seven absorbent pads as a waste reservoir to hold ~20 mL of liquid. We also use black porous filter membranes with 5 μm pore size as our cyst-capturing surface; this membrane has extremely low auto-fluorescence and facilitates the counting of *Giardia* cysts by increasing the contrast between the cysts and the membrane surface. In our cassette design, an additional filter membrane with 8 μm pore size is also used as a porous spacing layer and is placed below the black filter membrane to prevent backflow of particles to the cyst capture surface[19] (see Figure 2).

Prior to the assembly of the sample holder cassette, the absorbent pads are cut into square pieces (i.e., 4.1 cm × 4.1 cm) and patterned using a laser-cutting device (Versa Laser, Model No 2.30) to align the membranes and the tape onto the pad. We covered double-sided adhesive tape with a black masking tape and cut a hole with a diameter of one centimeter using the laser-cutter. We covered these tape pieces with five thin layers of black epoxy paint in order to decrease their auto-fluorescence and let them dry at room temperature under laminar airflow.

To assemble the sample cassette, we first place seven layers of absorbent pads into the lower casing of the sample holder cassette. The porous spacing layer is then immersed into the 0.01% Tween® 20 solution (prepared in reagent-grade water) and is placed on top of the upper absorbent pad. The black filter membrane is rinsed with isopropanol and deionized water to decrease the number of extractable objects on the membrane. Subsequently, the membrane is immersed into the 0.01% Tween® 20 solution to make it hydrophilic and is placed on top of the porous spacing layer. Then, the previous tape covered with epoxy paint is applied to the membrane to fix the position of the black membrane on the absorbent pad and to define the boundaries of the cyst capture area. Lastly, the disposable cassette is covered with the 3D-printed upper casing (Fig. 2a).

Water sample preparation

The sequence of steps for sample collection, labeling, filtration and optical imaging is summarized in Figure 2b. The method of direct labeling is used to label the *Giardia* cysts in the water sample with a fluorescent stain. First, 200 μL of the diluted stain is added to 10 mL of the water sample under test in a falcon tube and the tube is covered with aluminum foil to prevent light exposure. After mixing the sample gently for ~10 seconds, the sample is incubated at room temperature for ~35 minutes for labeling. To reduce the number of cysts adhering to the syringe barrel, a 10 mL syringe barrel is filled with 0.01% Tween® 20 solution and incubated at room temperature

for about 20 minutes. After removal of the Tween® 20 solution from the syringe barrel, the sample is poured into the syringe barrel with a Luer cap on the other end, the piston of the syringe is replaced, and the Luer cap subsequently removed. The water sample is then dispensed onto the black membrane until it is completely absorbed by the pads through capillary force, without the need for an electrically driven flow. To wash out the remaining sample in the sample tube, the tube is refilled with 5 mL of reagent-grade water and shaken vigorously for 15 s, and this tube liquid is then collected into the syringe and dispensed directly onto the filter membrane. This step is repeated twice to completely wash out the test tube. A total of 100 μL of washing buffer and 200 μL of counterstain (diluted in washing buffer at a 3:1 ratio) are then dispensed onto the cyst capture membrane. The counterstain is used to enhance contrast and to reduce the auto-fluorescence of the absorbent pad. Lastly, we cover the membrane with droplets of anti-fading mounting medium to decrease photo bleaching of the fluorescent stain. The total amount of time that is required for all these steps is less than 1 hour as detailed in Fig. 2b.

Design of the smartphone-based fluorescence microscope

Nokia Lumia 1020 is used in the design of our smartphone-based fluorescence microscope. This cell phone allows the capture of 38MP raw format (i.e., digital negative (DNG)) images at a 4:3 aspect ratio with a pixel size of 1.12 μm[20,21]. The built-in objective lens of the cellphone has a focal length, f of 7.2 mm and a relative aperture of f/2.2. Using the Nokia camera application settings, we are also able to adjust a variety of camera parameters (i.e., white balance, focus, ISO speed, exposure value, and contrast) for optimal image capture.

For fluorescence excitation, eight blue LEDs powered with two AA alkaline batteries are distributed evenly at each side to uniformly excite the cysts captured on the membrane of the sample holder (see Figure 1). The emission spectrum of each LED is also filtered using an excitation bandpass filter with a center wavelength of 470 nm and bandwidth of ~40 nm. An aspherized achromatic lens with a focal length, f_2 of 30 mm is used to create a magnification factor of 0.24 (i.e., f/f_2) between the sample plane and the CMOS sensor-chip of the mobile-phone, which helps us achieve a large sample FOV (~0.8 cm^2) per image, without any mechanical scanning. To adjust the depth of focus of our microscope we have placed a z-stage between the external lens and the excitation LEDs. To block the excitation light, a long-pass emission thin-film filter with a cut-off wavelength of 510 nm is placed between the existing cell phone lens and our external lens. The custom-designed opto-mechanical housing of our fluorescence microscope attachment is also 3D-printed (Stratasys, Dimension Elite) using ABS thermoplastic material.

Digital analysis of fluorescent images and automated cyst counting using machine learning

Digital image processing and machine learning algorithms are applied to detect and count *G. lamblia* cysts captured on the filter membrane as illustrated in Figure 3. In order to automatically detect and specifically count the cysts, the raw format (i.e., DNG) fluorescence image is uploaded to our servers using our *Giardia* Analyzer application (see Figure 3). On the server side, this DNG image is converted into TIFF format and the Bayer pattern image is retrieved. After a simple masking step, the inner part of the filter membrane image is cropped as our target region of interest (ROI). The green channel image of our ROI is then converted into a binary image based on a threshold value of 0.02 (maximum intensity: 1), following subtraction of the background intensity. The obtained

Fig. 3 Process flow for automated detection and counting of *G. lamblia* cysts using our custom developed smart application running on a Windows-based mobile phone. The processed image and cyst counting results are sent back to the mobile phone within less than ~2 minutes.

binary image contains not only the fluorescent particles (i.e., cyst candidates) but also noise. Our algorithm eliminates some of this noise related artifacts by discarding each connected component on the image that exhibits an area substantially smaller than the size of an intact *Giardia* cyst. For each one of the remaining cyst *candidates* within our ROI, we automatically generate a list of spatial features such as area, eccentricity, orientation, and equivalent diameter, among others. To increase the sensitivity of the differentiation of cysts from other (auto)fluorescent particles, we add more features to each particle's feature list by extracting intensity information (e.g., average intensity (I_{ave}), minimum intensity (I_{min}), and maximum intensity (I_{max})) of circular regions at each particle position with a three-pixel radius for not only the red, green, and blue channels of the RGB color space, but also their corresponding hue (H), saturation (S), value (V) of the HSV color space as well as the luma (Y), blue-difference (Cb) and red difference (Cr) of the YCbCr color space. Moreover, we include the differences of intensity parameters between each channel within a particular color space (e.g., $I_{ave,Y}$-$I_{ave,Cr}$, $I_{max,Y}$-$I_{max,Cr}$ or $I_{min,Y}$-$I_{min,Cr}$). This entire process creates a *71-item* feature list for each fluorescent particle (or cyst candidate) found within our filter ROI.

Next, we use a custom-developed machine learning algorithm to count and differentiate cysts from other unwanted (auto)fluorescent micro-objects in our filter ROI. This machine learning algorithm utilizes a bootstrap aggregating[22–24], or bagging, approach to classify particles using the 71 different features extracted for each cyst candidate[25]. Our training data that we used to train our machine learning approach to distinguish *Giardia* cysts from other micro-objects were populated by 14 different experiments of varying cyst concentrations for a total of 1370 cysts and 1485 other micro-particles. To create this training data/library, which need to be generated only once to statistically learn cyst images on our mobile microscope, each particle is labelled as either a cyst (or cluster of cysts) or other micro-object by manually determining the ground truth under a high-resolution bench-top microscope. Through this training process, we observed that the pixel area of the cyst clusters is proportional to the number of cysts that form the cluster,

based on which we generated a linear calibration curve, i.e., Pixel area = 10.34 × (Number of cysts) + 9.60, exhibiting a high correlation coefficient of 0.9808. This calibration curve is used to estimate the number of cysts in each fluorescent cluster/spot that is labeled as "cysts" using our machine learning algorithm.

After this training process, when detecting and counting *Giardia* cysts on new (i.e., blind) test images, fluorescent objects are automatically detected, noise-filtered, and the feature lists (each with 71 entries) for the remaining particles/candidates are digitally extracted as described above. Each set of features for a cyst or cluster candidate is compared against the training data automatically using our machine learning algorithm, classifying them as either *Giardia* cysts or other unwanted micro-objects. The final counting result is stored in our server database and is also wirelessly transferred to the smartphone through our custom developed application (Fig. 3).

Results and Discussion

Our waterborne pathogen detection platform has some distinct features that make it an ideal mobile analysis tool for rapid and automated imaging and detection of waterborne pathogens in resource limited settings: (1) The smartphone based fluorescence microscope has a large FOV of ~ 0.8 cm^2, which is more than an order of magnitude larger than the FOV of e.g., a 4× or 10× objective lens with a numerical aperture of ~0.1-0.2, making it possible to image the entire filter membrane surface without the use of a mechanical scanning stage; (2) the disposable sample cassette is capable of holding large volumes (e.g., 20 mL) of liquid sample and a further increase in this volume can be achieved by adding more layers of absorbent pads without a change in performance; and (3) its design is cost-effective and field-portable, weighing only 205 g, excluding the mobile-phone.

In order to blindly demonstrate the proof of concept of our mobile fluorescence microscope (Fig. 1), *G. lamblia* spiked water solutions were used as test samples. Each water sample was prepared

and processed according to the set of procedures described in Fig. 2 and our Methods Section. Fig. 4a shows a full FOV image captured
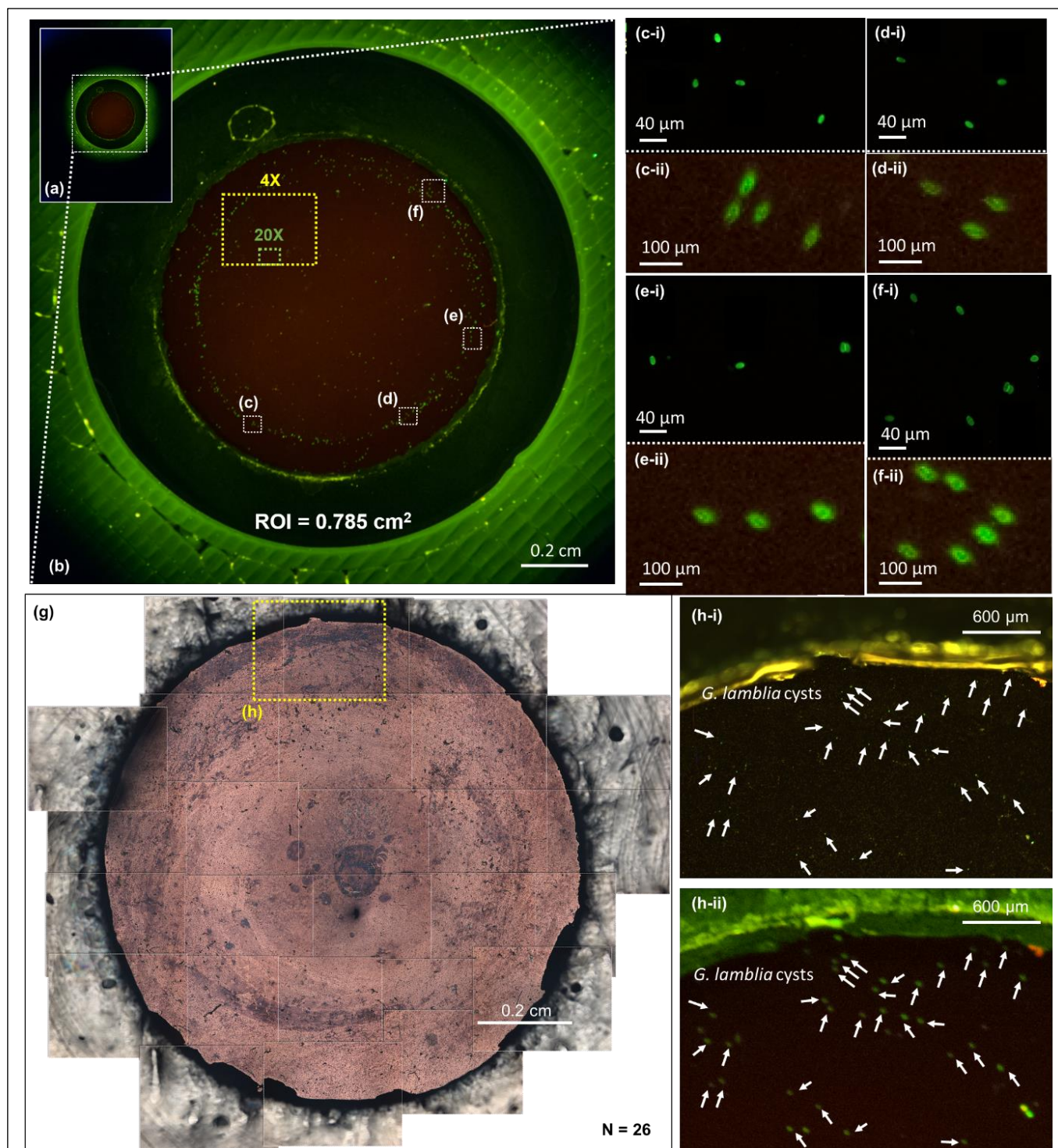
Fig. 4 (a) An image taken using our smartphone based fluorescent microscope. (b) Enlarged view of the region of interest in a single image taken using smartphone based fluorescent microscopy. (c, d, e, and f) (i) Comparison images taken using a 20× objective lens and a benchtop microscope with GFP filter (exposure time 5s and gain 1). (ii) Digitally cropped images taken using our smartphone based fluorescence microscope. (g) A comparison image showing the entire field of view of the filter membrane, which combines 26 different images taken using a 4× objective lens and a benchtop Olympus microscope under bright field illumination. This image is used for comparison purposes and illustrates the large FOV of our fluorescent microscope, shown in (b), compared to a standard benchtop microscope. (h) (i) Image taken using a 4× objective lens and a bench-top microscope with GFP filter (exposure time 20s and gain 1); (ii) Zoomed-in image taken using the smartphone based fluorescence microscope for the same region of interest on the filter membrane surface.
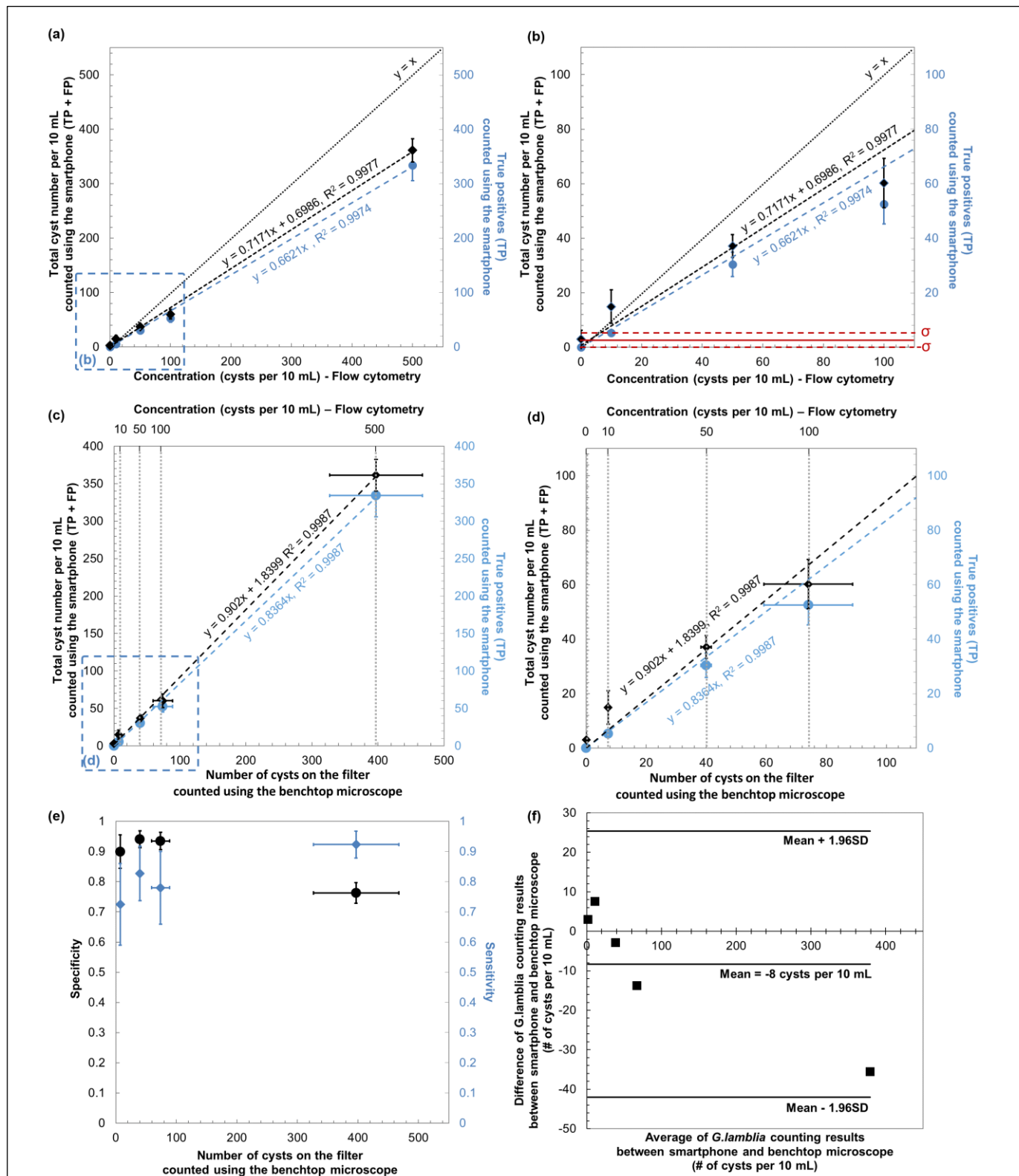
Fig. 5 Limit of detection (LoD), sensitivity and specificity of our smartphone-based *Giardia* analyzer determined using known concentrations of *Giardia* at 0, 10, 50, 100, and 500 cysts/mL. Each concentration is measured 3 times. (a) Our cyst recovery rate as a function of the cyst concentration, where y = x line defines the ideal recovery curve (100% recovery). (b) Zoomed in version of (a). (c) A plot demonstrating the accuracy of our machine learning based cyst counting algorithm. (d) Zoomed in version of (c). (e) The sensitivity of our machine learning algorithm is shown. Sensitivity = TP / (TP+FN), where TP and FN refer to True Positives and False Negatives, respectively. The specificity of our machine learning algorithm is shown. Specificity = TN / (TN+FP), where TN and FP refer to True Negatives and False Positives, respectively. (f) The Bland-Altman analysis, comparing smartphone-based measurement results against the results of a benchtop fluorescence microscope.

using our smartphone-based fluorescence microscope. In the zoomed-in image, shown in Fig. 4b, the filter membrane that captures the cysts in the water sample forms the inner circle, the black masking tape forms the middle circle, and the center part of the upper casing of the sample holder forms the outer part. The cyst ROI, i.e., the filter membrane with 5 μm pores, has an imaging area of ~0.8 cm^2. 26 different images taken with a 4× objective lens on a regular bench-top microscope were digitally stitched together to create a comparison image for this large FOV (as shown in Figure 4g – which is only used for comparison purposes). The insets of Fig. 4b (i.e., the regions marked as c, d, e, and f) and Fig. 4g (i.e., the region marked as h) illustrate the performance of this mobile platform. Panels labeled with (i) in Figures 4c-4f and Figure 4h show the images obtained using 20× and 4× objective lenses, respectively, of a regular bench-top fluorescence microscope to provide verification for (ii)-labeled images that were cropped from the digital image taken using our mobile fluorescence microscope. These cropped mobile-phone images are in good agreement with conventional bench-top microscope images that were captured for comparison, and individual as well as clustered cysts can be imaged using our mobile microscopy platform.

To explore the detection limit, sensitivity and specificity of our mobile-phone based cyst detection and quantification approach, we used flow-cytometer enumerated *G. lamblia* spiked water samples, each 10 mL in volume. Figure 5 summarizes the results of these experiments, which were based on five different cyst concentrations (i.e., 0, 10, 50, 100, and 500 cysts per 10 mL), with each experiment blindly verified using a bench-top fluorescence microscope, scanning >25 different ROIs across the filter membrane surface.

Although on average 79% of *G. lamblia* cysts that existed in our water sample volume (10 mL) were physically captured on the filter membrane, we achieved a lower overall cyst recovery as illustrated in Figs. 5a-b. The cyst detection efficiency of our system is influenced by two independent factors: (1) the partial loss of *Giardia* cysts during the delivery of the water volume of interest onto our disposable filter membrane; and (2) inaccurate detection and counting of the captured fluorescent objects on the membrane surface by our machine learning algorithm. The second issue is partially affected by difficulties in digitally differentiating the cysts captured at the outer edges of the filter membrane, which exhibit stronger auto-fluorescence arising from ABS material of the sample cassette. Based on Figs. 5c-d, we can quantify the overall sensitivity (i.e., Sensitivity = TP / (TP+FN), where TP and FN refer to True Positives and False Negatives, respectively[26]) of our machine learning algorithm as ~84%. In other words, the *Giardia* cysts that are physically captured on the filter membrane can be counted with an average sensitivity of ~84% using our machine learning based cyst detection algorithm (also see Fig. 5e for our detection sensitivity values for different cyst concentrations).

The LoD of our waterborne parasite imaging platform can be estimated as ~12 *Giardia* cysts per 10 mL based on the mean cyst count for the control samples plus 3 times their standard deviation [27] (see Figures 5a and 5b). Furthermore, the specificity of our detection method, (i.e., Specificity = TN / (TN+FP), where TN and FP refer to True Negatives and False Positives, respectively[26]), can be measured as 90%, 94%, 94%, and 76% for 10, 50, 100, and 500 cysts per 10 mL samples, respectively (see Fig. 5e). We further compared the performance of our smartphone based detection platform against a benchtop microscope using the Bland-Altman analysis, which shows a bias of -0.8 cysts per mL, with 95% confidence intervals of -4.2 cysts per mL and 2.5 cysts per mL (Figure 5f). These results illustrate the success of our machine learning based mobile microscopy platform to sensitively and specifically detect and

digitally separate cysts from other unwanted micro-objects that are captured on the filter membrane.

To further improve our overall cyst detection performance, we can target the recovery of the cysts that are lost during the transfer of the water from the sample container onto the porous filter surface. Potential mechanisms for this partial loss of intact *Giardia* cysts in our sample processing steps include: (i) rupture of the cysts due to mechanical forces and the negative pressure that build up during the processing of the water sample; (ii) non-specific binding of the cysts to the syringe barrel surface or the Luer cap; (iii) dead liquid volumes that remain in our sample delivery scheme, which might function as reservoirs/traps for some *Giardia* cysts; and (iv) uncontrolled pore size variations or non-uniformities on the filter membrane which might allow some cysts to pass through the pores. Through a systematic study of these potential sources of cyst losses, we believe that we can further improve our cyst capture efficiency on the filter membrane to >85-90% from its current value of 79%. We can also improve the robustness of our detection platform against dirt and undesired large particles/objects that might be found in natural water sources using a pre-filtration system. To handle such dirty natural water sources and still be able to achieve ~1 cyst/mL level of detection limit, we can utilize a series of larger pore filter membranes, where at each stage the pore size is gradually decreased, for example from 100 μm to 50 μm and then to ~25 μm, before the membrane filters that are employed in our current sample holder design are used.

In terms of specificity and sensitivity of cyst detection, our machine learning algorithm utilizes a bagging approach to classify particles either as a cyst or other micro-object using 71 different fluorescent image parameters as detailed in our Methods Section, and it was trained with mobile-phone based *Giardia* images captured over a wide range of experiments, involving 1370 individual *Giardia* cyst images. To further improve the performance of our machine learning code, we can expand this cellphone based *Giardia* image library by capturing e.g., >10,000 individual *Giardia* cyst images using our mobile microscope. This significant increase in our gold-standard image database/library should assist us in digitally boosting our specificity and sensitivity analysis for the fluorescent objects that are captured on our filter membrane area. Especially, this larger training dataset of *Giardia* cyst images should better handle some of our current challenges in automated identification/recognition of the cysts that are captured at or close to the outer edges of the filter membrane, which contain some auto-fluorescence signal due to the 3D printed plastic material.

Conclusion

We introduced a hand-held and cost-effective mobile imaging platform that is coupled with machine learning for automated detection and enumeration of *G. lamblia* cysts in large volumes of water. This platform includes a smartphone-based fluorescence microscope for imaging custom-designed disposable water sample cassettes that capture fluorescently labeled *Giardia* cysts over a wide filter surface area (~0.8 cm^2). A fluorescence image of the entire filter area is captured and transferred to our servers using the smartphone over a wireless network for remote digital processing to automatically detect and count the *Giardia* cysts captured on the filter membrane. The result of this machine learning based analysis is transferred back to the smartphone within 2 minutes using our custom-developed Windows phone application. Using flow-cytometer-enumerated *Giardia* spiked water samples, we demonstrated that this platform achieves a LoD of ~12 cysts per 10 mL, where each experiment takes ~1 hour, including all the steps of sample preparation and analysis. This portable system is a promising

tool for rapid and cost-effective on-site water quality monitoring and spatio-temporal analysis in resource-limited regions. We also believe that this machine learning based mobile fluorescent imaging and detection platform can be further useful for screening of biological liquids of interest (e.g., blood and urine) and for detection and quantification of various pathogens including e.g., bacteria, parasites, and eggs of parasites.

Acknowledgements

Conflicts of Interest Statement

A.O. is the co-founder of a company (Holomic LLC) that commercializes computational microscopy, sensing and diagnostics tools.

Notes and references

[a] Department of Electrical Engineering, University of California Los Angeles (UCLA), CA 90095, USA.

[b] Department of Bioengineering, University of California Los Angeles (UCLA), CA 90095, USA.

[c] California Nanosystems Institute (CNSI), University of California Los Angeles (UCLA), CA 90095, USA.

*Correspondence to: Prof. Aydogan Ozcan (UCLA Electrical Engineering and Bioengineering Departments, Los Angeles, CA 90095; Tel: +1 (310) 825-0915; E-mail: ozcan@ucla.edu; http://www.innovate.ee.ucla.edu; http://org.ee.ucla.edu/)

1   WHO. Water Quality and Health Strategy 2013-2020 http://www.who.int/water_sanitation_health/publications/2013/water_quality_strategy.pdf?ua=1 (accessed Oct 1, 2014).

2   WHO. Progress on sanitation and drinking-water - 2014 update http://www.who.int/water_sanitation_health/publications/2014/jmp-report/en/ (accessed Oct 1, 2014).

3   Worldbank. World Development Indicators 2014 data.worldbank.org/sites/default/files/wdi-2014-book.pdf (accessed Oct 1, 2014).

4   WHO. Water Sanitation Health - Water related diseases http://www.who.int/water_sanitation_health/diseases/diarrhoea/en/ (accessed Oct 1, 2014).

5   Chen, Y.-F.; Jiang, L.; Mancuso, M.; Jain, A.; Oncescu, V.; Erickson, D. Nanoscale 2012, 4, 4839–4857.

6   Baldursson, S.; Karanis, P. Water Res. 2011, 45, 6603–6614.

7   Adam, R. D. Clin. Microbiol. Rev. 2001, 14, 447–475.

8   EPA. Method 1623.1: Cryptosporidium and Giardia in Water by Filtration/IMS/FA; 2012.

9   Baque, R. H.; Gilliam, A. O.; Robles, L. D.; Jakubowski, W.; Slifko, T. R. Water Res. 2011, 45, 3175–3184.

10   Bridle, H.; Kersaudy-Kerhoas, M.; Miller, B.; Gavriilidou, D.; Katzer, F.; Innes, E. A.; Desmulliez, M. P. Y. Water Res. 2012, 46, 1641–1661.

11   Keserue, H.-A.; Füchslin, H. P.; Egli, T. Appl. Environ. Microbiol. 2011, 77, 5420–5427.

12   Keserue, H.-A.; Füchslin, H. P.; Wittwer, M.; Nguyen-Viet, H.; Nguyen, T. T.; Surinkul, N.; Koottatep, T.; Schürch, N.; Egli, T. Environ. Sci. Technol. 2012, 46, 8952–8959.

13   Koehler, A. V; Jex, A. R.; Haydon, S. R.; Stevens, M. A.; Gasser, R. B. Biotechnol. Adv. 2014, 32, 280–289.

14   Lee, S. A.; Erath, J.; Zheng, G.; Ou, X.; Willems, P.; Eichinger, D.; Rodriguez, A.; Yang, C. PLoS One 2014, 9, e89712.

15   Mudanyali, O.; Oztoprak, C.; Tseng, D.; Erlinger, A.; Ozcan, A. Lab Chip 2010, 10, 2419–2423.

16   Rhodes, E. R.; Villegas, L. F.; Shaw, N. J.; Miller, C.; Villegas, E. N. J. Vis. Exp. 2012, 1–6.

17   Zhu, H.; Isikman, S. O.; Mudanyali, O.; Greenbaum, A.; Ozcan, A. Lab Chip 2013, 13, 51–67.

18   Ozcan, A. Lab Chip 2014, 14, 3187–3194.

19   Vonk, G. P. Test Device Including Flow Control Means. US5185127, 1993.

20   Wei, Q.; Qi, H.; Luo, W.; Tseng, D.; Ki, S. J.; Wan, Z.; Bentolila, L. A.; Wu, T.; Sun, R.; Ozcan, A. ACS Nano 2013, 7, 9147–9155.

21   Wei, Q.; Luo, W.; Chiang, S.; Kappel, T.; Mejia, C.; Tseng, D.; Chan, R.; Yan, E.; Qi, H.; Shabbir, F.; et al. ACS Nano 2014. DOI: 10.1021/nn505821y

22   Larranaga, P.; Calvo, B.; Sanatana, R.; Bielza, C.; Galdiano, J.; Inza, I.; Lozano, J.; Armananzas, R.; Sanatafe, G.; Perez, A.; et al. Brief. Bioinform. 2006, 7, 86–112.

23   Quinlan, J. R. In Proceedings of the Thirteenth National Conference on Artificial Intelligence and the Eigth Innovative Applications of Artificial Intelligence Conference; 1996; pp. 725–730.

24   Tan, A. C.; Gilbert, D. Appl. Bioinformatics 2003, 2, 1–10.

25   Mjolsness, E.; DeCoste, D. Science 2001, 293, 2051–2055.

26   Zou, K. H.; O'Malley, A. J.; Mauri, L. Circulation 2007, 115, 654–657.

27   Zhu, H.; Sikora, U.; Ozcan, A. Analyst 2012, 137, 2541–2544.

Lab on a Chip Accepted Manuscript